







Review

# Recent Advances in Optical, Electrochemical, and Field Effect pH Sensors

Federico Vivaldi <sup>1,2</sup>, Pietro Salvo <sup>2,\*</sup>, Noemi Poma <sup>1</sup>, Andrea Bonini <sup>1</sup>, Denise Biagini <sup>1</sup>, Lorenzo Del Noce <sup>1</sup>, Bernardo Melai <sup>1</sup>, Fabio Lisi <sup>3</sup> and Fabio Di Francesco <sup>1,4</sup>

- <sup>1</sup> Department of Chemistry and Industrial Chemistry, University of Pisa, Via Giuseppe Moruzzi 13, 56124 Pisa, Italy; federicomaria.vivaldi@phd.unipi.it (F.V.); n.pomasajama@studenti.unipi.it (N.P.); andrea.bonini@phd.unipi.it (A.B.); denisebiagini@virgilio.it (D.B.); Lorenzo.delnoce95@gmail.com (L.D.N.); melai@ccci.unipi.it (B.M.); fabio.difrancesco@unipi.it (F.D.F.)
- <sup>2</sup> Institute of Clinical Physiology (IFC) of National Research Council (CNR), Via Moruzzi 1, 56124 Pisa, Italy
- <sup>3</sup> School of Chemical Engineering and Australian Centre for NanoMedicine, University of New South Wales, Sydney 2052, Australia; fabio.lisi.lj@gmail.com
- <sup>4</sup> National Interuniversity Consortium for Materials Science and Technology (INSTM), Via G. Giusti, 9, 50121 Firenze, Italy
- \* Correspondence: pietro.salvo@ifc.cnr.it; Tel.: +39-050-3152703

**Abstract:** Although its first definition dates back to more than a century ago, pH and its measurement are still studied for improving the performance of current sensors in everyday analysis. The gold standard is the glass electrode, but its intrinsic fragility and need of frequent calibration are pushing the research field towards alternative sensitive devices and materials. In this review, we describe the most recent optical, electrochemical, and transistor-based sensors to provide an overview on the status of the scientific efforts towards pH sensing.



**Citation:** Vivaldi, F.; Salvo, P.; Poma, N.; Bonini, A.; Biagini, D.; Del Noce, L.; Melai, B.; Lisi, F.; Francesco, F.D. Recent Advances in Optical, Electrochemical, and Field Effect pH Sensors. *Chemosensors* **2021**, *9*, 33. <https://doi.org/10.3390/chemosensors9020033>

Academic Editor: Núria Serrano  
Received: 7 January 2021  
Accepted: 4 February 2021  
Published: 5 February 2021

**Publisher's Note:** MDPI stays neutral with regard to jurisdictional claims in published maps and institutional affiliations.



**Copyright:** © 2021 by the authors. Licensee MDPI, Basel, Switzerland. This article is an open access article distributed under the terms and conditions of the Creative Commons Attribution (CC BY) license (<https://creativecommons.org/licenses/by/4.0/>).

**Keywords:** pH; pH sensors; optical pH sensors; voltammetric pH sensors; potentiometric pH sensors

## 1. Introduction

The activity of the hydrogen cation plays an important role in a variety of large- and small-scale processes, ranging from industry to microbial life [1,2]. The measurement of the hydrogen cation concentration is a routine procedure in several fields, such as production control to guarantee the quality and durability of many industrial products, and clinical analysis during sample management and testing. For example, in the pharmaceutical industry, pH control makes the synthesis processes and pharmacokinetics analyses accurate and safe [3], whereas in the clinical field, it can be applied for the monitoring of chronic wounds [4,5], discrimination between healthy and tumor cells [6], and monitoring of exposure to pollution of street traffic-controllers and office-workers [7]. This wide application of pH measurement motivates the scientific research to find new methods and devices that can adapt to different scenarios.

The glass electrode, one of the very first systems to measure pH, is nowadays the gold standard. The first model was proposed in 1909 by F. Haber and Z. Klemensiewicz following the results obtained by M. Cremer, who, in 1906, noticed a potential difference across a thin glass membrane that separated two solutions with different pH values [8]. The most common model of the glass electrode consists of an inner Ag/AgCl reference electrode separated from another Ag/AgCl electrode by a glass membrane. One electrode is in contact with a known pH solution while the other with an unknown pH sample. An overall electric potential difference ( $E_m$ ) across the membrane appears because the silicate network has an affinity for specific cations, which are adsorbed within the structure.  $E_m$  is the sum of contributions from the junctions between the various zones of the glass electrode, including terms, such as the interfacial potentials arising from adsorbed cations, diffusion potentials within the glass membrane, and the asymmetry potential (generated

by the natural inhomogeneity of the membrane due to its construction or wear during use). Glass membranes are mostly selective for  $\text{H}_3\text{O}^+$ , but they also respond to other ions, such as  $\text{Na}^+$ ,  $\text{Li}^+$ ,  $\text{K}^+$ ,  $\text{Ag}^+$ , and  $\text{NH}_4^+$ .

Figure 1A shows a typical glass electrode. Despite its proven reliability, a glass electrode suffers from several drawbacks, such as frequent calibrations to compensate for the drifts caused by the asymmetry potential, and the intrinsic fragility of the glass membrane, which can degrade because of continuous measurements or harsh environments (e.g., reactors, biosystems, or in vivo applications).

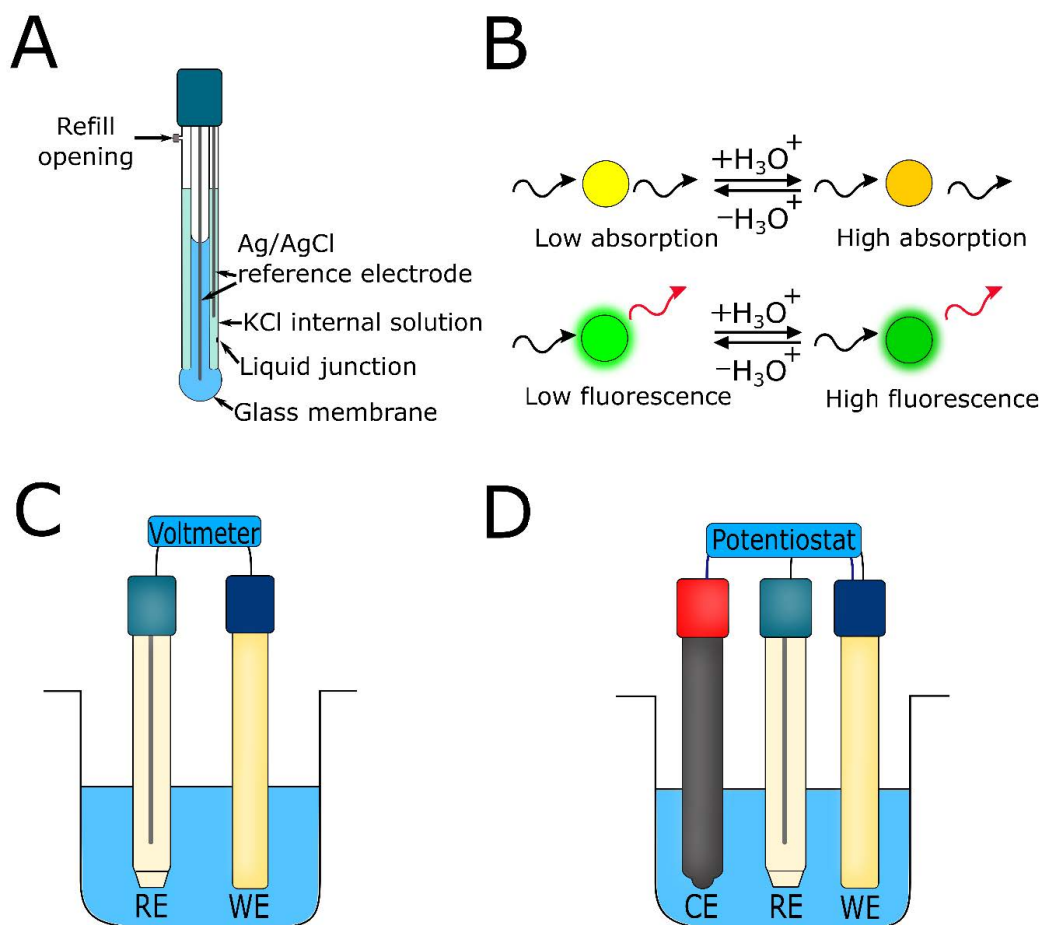


**Figure 1.** (A) Schematic representation of a cell with a glass electrode. Two Ag/AgCl electrodes are immersed in two solutions (with known and unknown pH values, respectively) and separated by a glass membrane. The electrical potential difference between the two electrodes is correlated to the pH of the unknown solution. (B) Schematic representation of the principle of optical transduction in an optical pH sensor based on absorption and fluorescence. (C) Schematization of a 2-electrode system inside a solution of a given analyte. (D) Schematization of a 3-electrode system for a voltammetric measurement.

In this review, we discuss the most promising pH sensors reported in the literature: optical and electrochemical sensors, and field effect transistors (FETs). Optical pH sensors typically use chemical species that modify their optical properties as a function of pH (e.g., index of refraction, polarization, absorbance, etc.) [9–12]. For example, Figure 1B shows a pH-sensitive species that changes its UV-VIS absorbance or its fluorescence emission depending on the protonation equilibrium. Electrochemical pH sensors are mainly potentiometric and voltammetric. Potentiometric sensors measure the potential generated across two electrodes, i.e., the working electrode (WE) and the reference electrode (RE) (Figure 1C). Voltammetric sensors measure the current generated when a potential is

imposed in an electrochemical cell through a three-electrode system with WE, RE, and a counter electrode (CE) that supplies current to the cell (Figure 1D). ISFETs (ion-sensitive field effect transistors) detect the change of the electrical field caused by hydrogen ions that modulate the current flowing in the transistor conduction channel. ISFETs' popularity depends on their microscopic size and potential high sensitivity towards pH [12,13].

## 2. Optical pH Sensors

Optical pH sensors are mostly based on sensitive acidic/basic materials with a specific  $pK_a$ , a high molar extinction coefficient, absorbance and emission spectra in the visible range, and good stability against light and a chemical environment (e.g., photostability and chemostability) [14]. A common approach is to immobilize a molecular probe with a chromophore on two types of supports, i.e., optical fibers and planar sensors. Optical fibers are flexible, can achieve a microscopic spatial discrimination, and can be quite easily modified. However, they are limited by ionic strength interferences and the photodegradation and leakage of the chromophore [15–18]. Planar sensors are easily fabricated and usually have a simple structure with a large pH-sensitive area [19–22].

In 2000, Jin et al. reported a sensor based on a polyaniline (PANI) film prepared by chemical oxidation at room temperature [23]. The different protonation of the imine nitrogen ion of PANI led to a pH-dependent behavior in the UV-VIS-NIR spectrum. The PANI film was deposited onto a planar plexiglass surface and showed an absorbance shift at 575 and 750 nm, which allowed pH to be measured in the range 2–12. Although this study reported promising data on the temporal stability of PANI, it did not show its application in real matrices. In addition, the presence of a hysteresis effect made this sensor incompatible for a continuous monitoring in wide ranges of pH.

In another study, Kermis et al. proposed a rapid method for the preparation of a sensor based on a fluorescent dye in a matrix obtained by copolymerization of 6-methacryloyl-8-acid hydroxy-1,3-pyren sulfonic with polyethylene-glycol acrylate [24]. The choice of these two polymers stems from their excellent mechanical properties and the possibility to directly immobilize a dye inside the matrix during the polymerization phase. Although the planar sensor showed a small operating range between pH 6 and 9, the reproducibility was high ( $<0.10$  pH units) and the dependence on ionic strength had a negligible effect (residual standard deviation, RSD  $< 3.6\%$ ). Stahl et al. followed a similar approach [21] and embedded a fluorescent pH-sensitive molecule, 2',7'-dihexyl-5(6)-*N*-octadecyl-carboxamidofluorescein ethyl ester, in a hydrogel matrix (polyurethane hydrogel "Hydromed D4") with a fluorescent standard (ruthenium(II)-Tris-4,7-diphenyl-1,10-phenanthroline). This setup was used to measure pH in 2-D marine sediments in the pH range 7.3–9.3 (Figure 2A). The concept of spatial measurements for marine samples has also been studied in the pH range 6–8 by Jiang et al., who used a fluorescent pH indicator (5-Hexadecanoylamino-fluorescein) and Hydromed D4 [22]. Recently, Gotor et al. designed several fluorescent dyes (boron–dipyromethene derivatives) embedded in Hydromed D4 to build an optical array capable of extending the pH measurements to a wide pH range (0–14) [25].

In 2012, Raoufi et al. reported a polyallylamine hydrochloride as a linker for a dye, "Brilliant Yellow", covering the tip of an optical fiber [26]. The polymer was deposited using the layer-by-layer technique, which allows for fine control of the polymer deposition on a solid surface by applying layers with opposite charge. The best sensitivity of the prototype was obtained in a range between pH 6.8 and 9 with an accuracy of 0.2 pH units.

In 2016, Abu-Thabit et al. described a similar system, which measured the pH response of polysulfone membranes coated with PANI nanofibers [27]. The nanoscale PANI structure improved the diffusion of molecules into the nanofiber and provided a response time of 4 s over a pH range from 4 to 12 with a standard deviation ranging from 0.002 to 0.05 pH units. The sensor was also tested in a detergent (Dettol brand), obtaining a relative error of about 1%. Although this sensor was tested for repeatability and was described to work flawlessly from week to week, no numerical data was reported.

Safavi et al. immobilized two dyes, “Victoria Blue” and dipicryamine (pKa 1.82 and 11.2, respectively), onto optically transparent triacetyl-cellulose membranes [28]. The authors used a neural network to extend the measurement range and obtained a sensor that performed better than a glass electrode in extreme pH conditions (RSD < 2% at pH 0–1 and 13–14). In 2006, Hashemi et al. immobilized a “Congo Red” dye on agarose membranes [29]. Although it had high precision (RSD < 0.30%), the sensor had a response time of about 3 min and could only be used in the acidic range (pH 0.5–5). Taweetanavanich et al. described a rhodamine-based colorimetric and fluorimetric sensor that worked between pH 1 and 8 [30]. The interference of several metal cations ( $\text{Na}^+$ ,  $\text{K}^+$ ,  $\text{Ag}^+$ ,  $\text{Mg}^{2+}$ ,  $\text{Ca}^{2+}$ ,  $\text{Pb}^{2+}$ ,  $\text{Ni}^{2+}$ ,  $\text{Cu}^{2+}$ ,  $\text{Zn}^{2+}$ ,  $\text{Cd}^{2+}$ ,  $\text{Hg}^{2+}$ ,  $\text{Al}^{3+}$ ,  $\text{Cr}^{3+}$ ,  $\text{Fe}^{3+}$ ,  $\text{Au}^{3+}$ ,  $\text{Pt}^{2+}$ ,  $\text{Ru}^{2+}$ ) was negligible, thus confirming the selectivity of the sensor towards the hydronium ion. However, the article did not mention any data regarding repeatability, reproducibility, and sensitivity.

In 2013, Li et al. removed the core from a section of an optical fiber and dip-coated the corresponding cladding with a pH-sensitive layer made of tetraethylorthosilicate (TEOS) and a mixture of pH-sensitive dyes (cresol red, dichlorophenol red, bromophenol blue) (Figure 2B) [31]. The core removal increased the power of the evanescent wave [32]. This sensor showed a linear response in the pH range 1–13 with a sensitivity of 0.6 dBm/pH, a response time of 40 s, and high repeatability (RSD < 1%). In a study from 2014 by Schyrr et al., the core of an optical fiber was coated with organic modified silicates (ORMOSILs) doped with bromophenol blue [33]. This sensor showed a sigmoidal response between pH 3 and 9 with a linear range between 5 and 7. The response time was 20 min for a pH variation of 1 unit. This sensor was tested in human serum samples and had an accuracy of 0.2 pH when compared with a glass pH meter. Another example of sol-gel technology was presented by Sørensen et al., who entrapped two dyes within a sol-gel matrix, which allows the rapid diffusion of protons [34]. Such a sensor worked in a range between 4.7 and 7.7 pH units with an accuracy < 0.1 pH units. Similarly, Jeon et al. used neutral red as a pH-sensitive dye, obtaining a device with a working pH range between 6 and 9 [35]. Vafi et al. proposed an optical absorption sensor based on a sol-gel silica matrix doped with thionines [36]. The sensor had a response time of about 1 min between 11 and 13 pH units with a lifetime of 6 months. Wencel et al. used a sol-gel-based optical pH sensor for real-time monitoring in human tissues [37]. The fluorescent dye 8-hydroxypyrene-1,3,6-trisulfonic acid was used to monitor pH between 6 and 8.5 and had a response time of less than 2 min.

Recently, Gong et al. proposed a fluorescent hydrogel-based optical fiber for lung tumors [38]. A fluorescent dye (5,10,15,20-Tetrakis(4-hydroxyphenyl)-21H,23H-porphine) was embedded in a polymeric matrix (4-hydroxybutylmethacrylate and dimethylaminoethylacrylate) and used to measure the pH (5.5–8) of ovine lung tissue within 30 s. Figure 2C shows another optical fiber sensor with a pH-sensitive hydrogel (acrylamide, *N,N'*-methylene diacrylamide, *N,N,N,N*-tetramethylethylenediamine, and methacrylic acid) [39]. A change in the volume and refractive index of the hydrogel caused by pH led to a shift in the surface plasmon resonance (SPR) wavelength. The highest sensitivity (13 nm/pH) was obtained in the range pH 8–10.

Moradi et al. injected a fluorescent pH-sensitive indicator (8-hydroxypyrene and 1,3,6-trisulfonic acid sodium salt) in a microfluidic serpentine (Figure 2D) [40]. The fluorescent signal was recorded in the pH range 2.5–9; however, the sensitivity was not constant but increased from 6 mV/pH at basic pH up to 42 mV/pH at acidic pH. The sensor had a response time of about 10 s with an optimal indicator concentration of 500 mg/L.

A different approach includes pH-sensitive inorganic materials, such as carbon nanostructures [41], metals (Ms), and metal oxides (MOs) [42–46]. Metallic materials can absorb hydronium ions or can form compounds with the general chemical formula  $\text{M}_x\text{O}_y\text{H}^+$  [47]. Because of the hydroxyl and carboxylic groups, reduced graphene oxide (rGO) is an excellent candidate for pH measurement [5,13]. An example was the deposition onto the unclad core of an optical fiber of a silver thin film coated with rGO and PANI [48]. The change in the refractive index increased with  $\text{OH}^-$  concentration; thus, the sensor had

a higher sensitivity at basic pH values (75.09 nm/pH at pH 11.35). In 2017, a metallic nanostructured complex ( $\text{ZnLi}_2$ ) was used in combination with sodium tetraphenylborate, dibutylphthalate, and polyvinyl chloride [49]. This absorbance sensor showed two linear ranges between pH 4 and 8 and between 5 and 8 depending on the wavelength (393 and 570 nm, respectively). The average response time was 4 min, with 1.14% measurement repeatability and 4.06% reproducibility. The sensor lifetime was more than 2 months when stored in water.

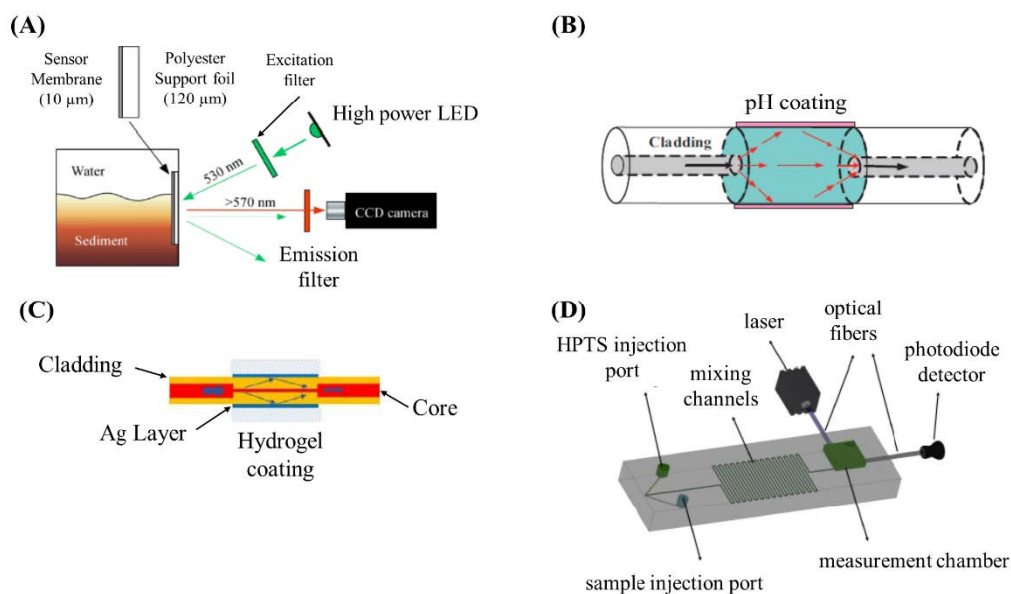


**Figure 2.** (A) Setup for spatial pH measurement of marine sediment (reprinted from [21] with the permission of Wiley). (B) Optical fiber without a core used for pH sensing (reprinted from [31] with the permission of Elsevier). (C) Hydrogel base fiber optic structure (reprinted from [39] with the permission of Elsevier). (D) Microfluidic device for pH measurements reported by Vahid et al. (reprinted from [40] with the permission of Elsevier).

Although there are some examples with inorganic materials, the most common optical pH sensors mainly consist of a dye embedded in a polymer. These sensors achieved a wide measurement range and, apart from some specific applications, such as the monitoring of human tissue, optical fibers are quite popular because they are relatively inexpensive and do not usually need a complex electronic readout system. However, there is the need for materials capable of reducing the leakage of the pH-sensitive optical species into the medium. Such research would allow for long-lasting sensors for pH monitoring.

### 3. Potentiometric pH Sensors

Potentiometric sensors measure the electrical potential between the WE and RE in a solution. The distribution of electric charge is a time-dependent phenomenon that is a function of several properties of the investigated system, e.g., the bulk composition, the composition of the sensitive layer, and the thermodynamic and kinetic properties [50].

Polymers are often used because they can be functionalized or embedded with pH-sensitive molecules. Lakard et al. studied the responses to pH of five different polymers (monomers: 1,3-diaminopropane, diethylene triamine, pyrrole, p-phenylene diamine, and aniline) electroplated on a platinum wire [51]. All sensors showed a linear response in the range pH 2–10, with the highest sensitivity of 52 mV/pH obtained for PANI films, close to that of the glass pH meter. The same authors used [52] photolithography to fabricate micro-supports for the electrodeposition of a polypyrrole film. This sensor proved that pH sensitivity depended on the polypyrrole thickness. A larger range was obtained from the fabrication of a pH-sensitive membrane by electropolymerization of poly-bis



phenol on an indium tin oxide electrode [53]. This method allowed robust systems to be fabricated with a sensitivity of around 57 mV/pH, a working range of 1–14 pH units, and a low interference from other common cations and anions ( $\text{Na}^+$ ,  $\text{K}^+$ ,  $\text{Cl}^-$ ,  $\text{SO}_4^{2-}$ ). These membranes were also tested in real matrices, such as milk and fruit juice. Guinovart et al. modified a commercial adhesive bandage for monitoring wound status. The sensor consisted of screen-printed Ag/AgCl tracks and an electropolymerized PANI WE. A polyvinyl butyral (PVB) membrane coated the RE to protect it against wound exudate (Figure 3A) [54]. The sensor worked in a physiological pH range (5.5–8 pH), and proved to have extremely efficient mechanical resistance, repeatability, and reproducibility of the measurements. The authors analyzed the sensitivity of the device after sterilization with an autoclave and observed a slight variation that depended on the glass transition of the membrane used as RE. A PANI nanofiber tested in buffer solution led to a superNernstian response (63 mV/pH) [55], whereas a slightly smaller sensitivity was obtained after coating gold interdigitated electrodes with PANI (58.57 mV/pH in the range pH 5.45–8.62, Figure 3B) [56].

One of the first examples of metallic-based potentiometric pH sensors used two forms of lead oxide to fabricate a pH-sensitive membrane on an aluminum substrate [57]. In the pH range 1–12, this sensor had a sensitivity of about 58 mV/pH with good repeatability (RSD < 2.7%) and was not affected from interferents, such as  $\text{Li}^+$ ,  $\text{Na}^+$ ,  $\text{Mg}^{2+}$ ,  $\text{Ca}^{2+}$ ,  $\text{NH}_4^+$ , and  $\text{HCO}_3^-$ . Manjakkal et al. proposed a potentiometric pH sensor based on ruthenium oxides and tantalum oxide as a pH-sensitive layer screen-printed on alumina substrates [58]. The sensors showed short response times (<15 s), long lifetime, sensitivities close to the Nernstian limit, and low interference towards metal cations, such as  $\text{Li}^+$ ,  $\text{Na}^+$ , and  $\text{K}^+$ . The sensor was tested in real matrices like lemon juice and river water, obtaining values close to commercial devices. Another superNernstian response in a potentiometric sensor was obtained by Khalil et al., who electroplated iridium oxide nanoparticles on a gold substrate [59]. This method led to a sensitivity of 73 mV/pH in a wide pH range (pH 1.68–12.36). Tanumihardja et al. used ruthenium oxide nanorods to fabricate an integrated sensor in an organ on chip system [60]. A near Nernstian sensitivity was achieved (58 mV/pH), with a short response time (2 s) and a drift of 0.013 pH/h. Choi et al. coupled tungsten oxide nanofibers with a dual-channel differential amplifier, which improved the signal-to-noise ratio and allowed the sensitivity to be increased to 377.5 mV/pH in the pH range 6.9–8.94 [61]. Crespo et al. used multi-walled carbon nanotubes (MWCNTs) in combination with an ion-selective membrane (tridodecylamine and potassium tetrakis [3,5-bis(trifluoromethyl)phenyl] borate in a methyl methacrylate and an n-butyl acrylate matrix) and achieved a good sensitivity of about 58 mV/pH, although the presence of  $\text{Li}^+$ ,  $\text{Na}^+$ ,  $\text{K}^+$ ,  $\text{NH}_4^+$ ,  $\text{Mg}^{2+}$ , and  $\text{Ca}^{2+}$  was noted [41]. Smith et al. proposed a combination of poly(3,4-ethylene-dioxythiophene)-poly(styrene sulfonate) (PEDOT:PSS), MWCNTs, and PANI on a flexible cotton yarn [62]. The yarn worked in a wide pH range (2–12) and in artificial sweat with an almost ideal sensitivity ( $61 \pm 2$  mV/pH).

Graphene and its derivatives have also been studied for potentiometric pH sensing [13,63,64]. Graphene oxide (GO) has several carboxylic, epoxy, and alcoholic functional groups that make it sensitive to pH changes. Melai et al. used GO for chronic wounds monitoring using a flexible support with screen-printed silver tracks and carbon WE. The sensor had a sensitivity of 31.8 mV/pH [65]. For clinical wound monitoring, Rahimi et al. proposed a pH sensor consisting of PANI deposited onto a combination of a laser-scribed polyimide sheet and a highly deformable ecoflex support [66].

Poma and coworkers decorated rGO with different organic molecules (4-aminobenzoic acid and 4-amino-phenylacetic acid) and improved the sensitivity up to 45 mV/pH in sea water, blood serum, and exudate [67–70]. A similar rGO-based sensor functionalized with 3-(4-aminophenyl)propionic acid was efficiently transferred on paper and tested against the same matrices (Figure 3C) [71]. Manjakkal et al. proposed a wearable pH sensor on a cellulose-polyester cloth coated with a polyurethane-graphite WE and an Ag/AgCl RE [72]. This sensor worked in the pH range 6–9 but had low sensitivity (4 mV/pH).

In 2009, Marxer et al. presented a sensor based on an Ag/AgCl electrode coated with a hybrid xerogel (aminosilanes/alkylsilane) of aminosilanes [73]. The working range was in the physiological pH range, whereas its sensitivity was amino silane dependent and ranged from 44 to 55 mV/pH.

The coupling of carbon-nanostructured material with a polymeric film was performed by Zuaznabar-Gardona et al., who electropolymerized a polydopamine film on a multi-layer carbon nano-onion substrate deposited on an glassy carbon electrode [74]. This composite demonstrated low interference from monovalent cations and a sensitivity close to that of the glass electrode. The device was capable of measuring pH in different matrices (milk, sea water, pineapple juice, and vinegar).

Sulka et al. proposed hydroquinone monosulfonate-doped polypyrrole nanowires and obtained a sensitivity of 46–49 mV/pH, which was not far from that of the glass electrode [75].

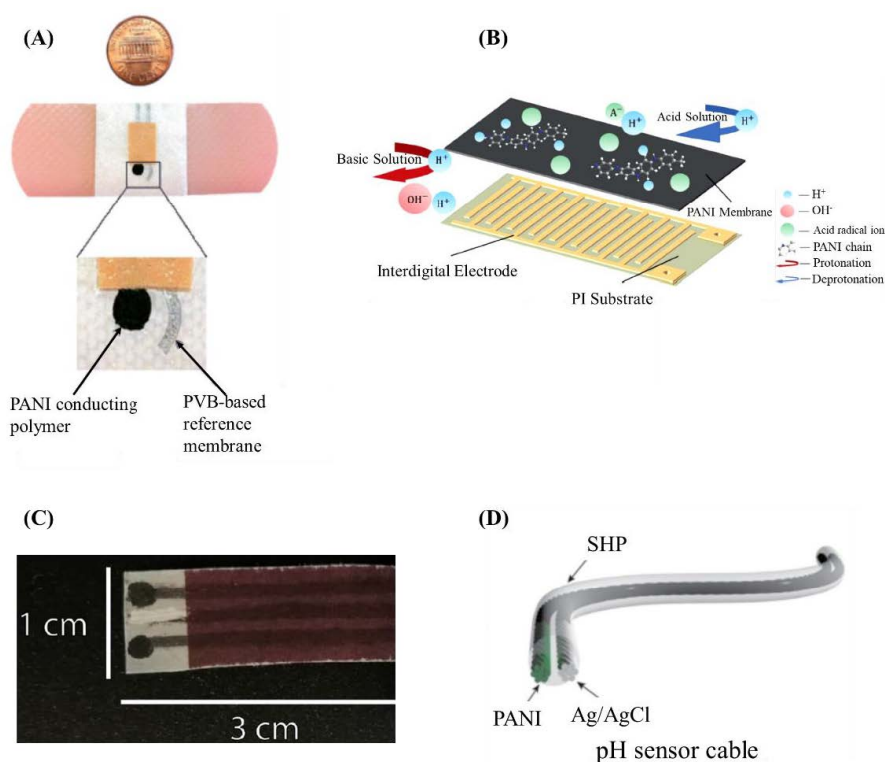


**Figure 3.** (A) PANI-based pH sensor for wound monitoring (reprinted from [54] with the permission of Wiley). (B) PANI-based interdigitate gold electrodes onto a polyimide (PI) substrate for pH sensing (reprinted from [56], published by The Royal Society of Chemistry). (C) Paper-based pH sensor using rGO functionalized with 3-(4-aminophenyl)propionic acid (reprinted from [71] with the permission of IEEE). (D) Self-healing PANI-based (SHP) pH sensor (reprinted from [76] with the permission of Elsevier).

Yoon et al. developed a remarkable pH sensor that consisted of two carbon fiber threads coated with a self-healing polymer (poly(1,4-cyclohexanedimethanol succinate-co-citrate)) (Figure 3D) [76]. One thread was coated with a PANI layer, whereas the other with Ag/AgCl as RE. The device showed an almost ideal sensitivity (58.1 mV/pH) with a 5-s response time in the range of pH 4–10. Furthermore, measurements were performed in real matrices (urine, saliva, sweat, and human tears) and results were comparable with those of a commercial pH meter.

#### 4. Voltammetric pH Sensors

Voltammetric pH systems are less common than potentiometric and optical chemical pH sensors because of the few suitable compounds for this type of transduction. These measurements usually depend on sensitive materials capable of involving hydrogen ions in the electrochemical reaction. Therefore, by measuring the current generated during the redox process, it is possible to establish a correlation with pH. In voltammetry, the sensitivity can be expressed as mV/pH since the current/potential profile, called a voltammogram, is often chosen to monitor pH.

Stred'Ansky et al. studied the redox quinone-hydroquinone pair, which was known to be pH dependent [77]. In 2002, Wildgoose et al. described a more accurate work, where carbon particles were covalently modified with anthraquinone and immobilized onto pyrolytic graphite electrodes [78]. This sensor had a sensitivity of about 58 mV/pH over a range of about 1 to 9 pH units. The article analyzed the effect of temperature on the sensor sensitivity in the range 20–70 °C, recording a variation consistent with the Nernst law. Makos et al. developed a carbon fiber microelectrode using the chemistry of para-quinone [79]. Although having the advantage of a miniaturized system, the sensor showed a low sensitivity, about 38 mV/pH, and a small working range (6.5 at 8 pH). Later, Amiri et al. electrodeposited polydopamine in aqueous solution onto glassy carbon electrodes [80]. As for quinone, polydopamine is involved in a two electron–two proton exchange process, which allows for the transduction of the H<sup>+</sup> concentration into current. The sensor showed a sensitivity of approximately 58 mV/pH in a range from 1 to 12 pH units with a reproducibility of 0.83%. Chaisiwamongkhol et al. reported a sensor based on porous graphitic carbon fibers functionalized with quinone groups [81]. This sensor had a superNernstian sensitivity of 65 mV/pH in the pH range 2 to 8 by performing scans on a potential range from −0.2 to 0.8 V. When tested in a real saliva sample, the performances were comparable with those of a glass electrode.

Recently, Vivaldi et al. fabricated a voltammetric pH sensor using an indoaniline derivative as a sensitive layer (Figure 4A) [82]. Exploiting the two electron–two proton reaction mechanism typical of quinones, this molecule allowed for pH measurement in low potential windows (−0.4–0.2 V) with a sensitivity of 56 mV/pH. This sensor experienced no leakage of the sensitive molecule in the medium thanks to the binding properties of the indoaniline derivative. Furthermore, the device was successfully used in biological samples (urine, saliva, and blood) and in beverages (orange juice, milk, and tea) with an accuracy better than 0.1 pH unit. Genotoxicity tests were carried out on the synthesized indoaniline derivative, proving the absence of genotoxic effects on living cells.

Chaisiwamongkhol et al. used a metal oxide (iridium oxide) for pH monitoring in blood samples [83]. This sensor had a sensitivity of about 63 mV/pH and high reproducibility (RSD < 2%) in the working potential range −0.2–0.8 V. In 2019, Tham et al. used riboflavin as a pH-dependent molecule and a vitamin E derivative as a pH-independent reference to fabricate a biocompatible pH sensor that proposed an alternative to the typical Ag/AgCl RE. Thanks to the reversible 2e<sup>−</sup>/2H<sup>+</sup> process in riboflavin, this sensor had a sensitivity of about 50 mV/pH in buffered media, whereas the response in unbuffered media was negligible because of the low concentration of localized H<sup>+</sup> (Figure 4B) [84].

pH-sensitive carbon materials were reported by Zhu et al., who fabricated a voltammetric pH sensor using an electrochemically modified nanocrystalline graphite-like amorphous carbon [85]. The application of positive voltage (2 V vs. an Ag/AgCl RE) in sulfuric acid allowed for the formation of pH-dependent quinonic groups on the carbon surface. This sensor had a superNernstian response of 63.3 mV and negligible effect from K<sup>+</sup> and Na<sup>+</sup>. However, the surface required electrochemical regeneration after 20 measurements. Hu et al. described a quinone-functionalized tryptophane for the development of a pH sensor on a graphite electrode [86]. Interestingly, this sensor could be used both in voltammetric and potentiometric modes, obtaining a sensitivity of 52 mV/pH in a wide pH range (1–12). A comparison with a glass electrode led to accurate measurements in complex matrices like milk and cola.



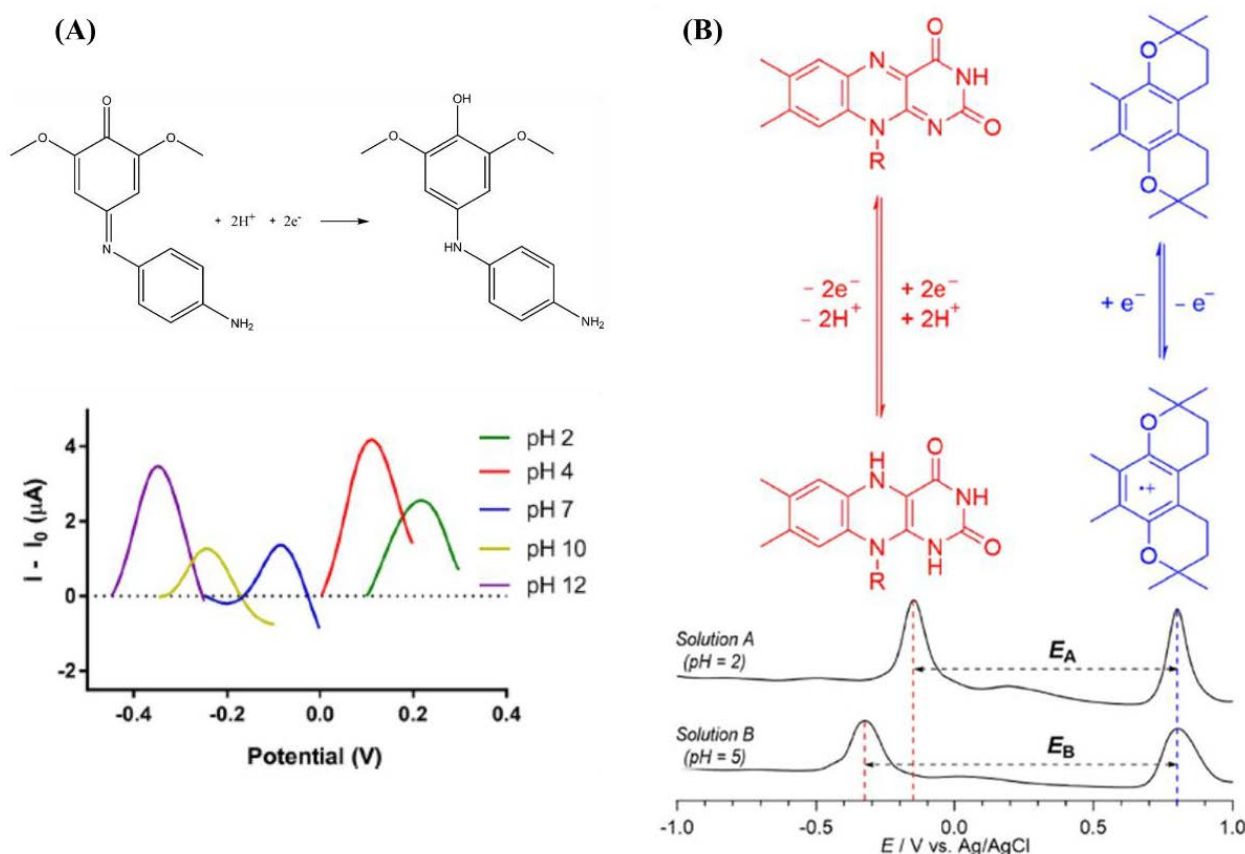


**Figure 4.** (A) Response of an indoaniline-based voltammetric pH sensor (reprinted from [82] with the permission of Elsevier). (B) Square wave voltammetry of the vitamin-based pH sensor (reprinted from [84] with the permission of Elsevier).

Instead of the potential, Gao et al. measured the current flowing in a PANI film electropolymerized onto a graphite electrode [87]. This sensor worked between 2 and 10 pH units; however, sensitivity was low. In another study, Sha et al. assessed by cyclic voltammetry the pH dependence of an electrodeposited PANI layer onto a graphene substrate [88]. The device showed two linear response ranges, one from pH 1 to 5, and a second from 7 to 11 with a sensitivity of about  $-50$  and  $139 \mu\text{A}/(\text{pH}\cdot\text{cm}^2)$ , respectively, with potential scans ranging from  $-0.25$  to  $1$  V. Further work is needed to assess whether this sensor can be used as a linear pH sensor in the full range.

### 5. pH Sensors Based on Field Effect Transistors

An ISFET is capable of transducing the  $\text{H}^+$  concentration into a current via the field effect [13], which depends on the interaction between an  $\text{H}^+$ -sensitive layer deposited onto the gate. The gate is often removed and the solution under measurement becomes the gate. These devices are easily miniaturized and mass-produced, and have proven to be effective in the quantitative measurement of analytes as early as 1970 [89].

At the beginning of the 2000s, a mix of tin oxide and metallic aluminum was used as the gate [90]. This ISFET showed a sensitivity of about  $58 \text{ mV}/\text{pH}$  working in a pH range from 2 to 10. However, the article did not analyze any other analytical parameter since it focused on the study of the sensor's electro-technical apparatus.

In 2002, Shitashima et al. fabricated an FET using  $\text{SiO}_2/\text{Si}_3\text{N}_4$  as a pH-sensitive gate insulator, which was coupled with an ion-sensitive electrode for the chloride ion to monitor marine pH [91]. The article only reported the calibration method and the results in real matrices. In another paper, a microfluidic system was used to supply standard pH solution for the calibration of an ISFET that measured marine pH [92]. Rani et al. developed an ISFET by changing the type of gate from single to "multi finger" to improve the transistor

performances [93]. However, the sensitivity was rather low (about 45 mV/pH) and the response time was long (600 s).

Parizi et al. obtained a superNernstian response using an ISFET based on an aluminum oxide layer deposited on an aluminum extended gate [94]. A remarkable sensitivity of 130 mV/pH was achieved in the range pH 4–10. In 2014, Das et al. proposed a superNernstian pH (62 mV/pH) sensor using an EGFET (extended gate field effect transistor) with palladium oxide (Figure 5A) [95]. The EGFET worked in the pH range 2–12, with a hysteresis of about 7.4 mV. The drift was 2.4 mV/h.

Cho et al. fabricated an extended gate of indium tin oxide further covered with a layer of tin oxide on paper [96]. The device showed a sensitivity of 57 mV/pH in the range pH 4–10. This study demonstrated the feasibility of the integration into systems that aim to be more environmentally friendly than classic silicon-based systems.

An article by Kang et al. reduced the RE noise coupling an ISFET with an REFET (reference field effect transistor), which has low pH sensitivity [97]. Integrating a platinum RE, the fluctuation of the solution potential was removed by a differential measurement between the ISFET and the REFET.

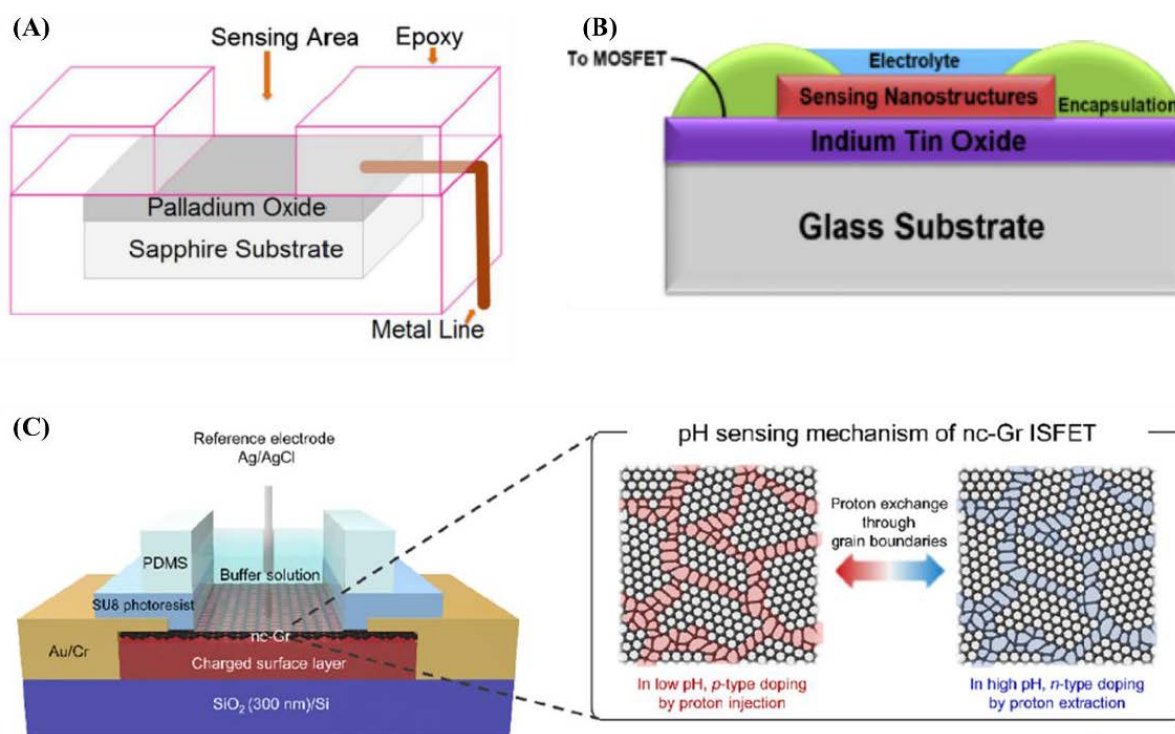


**Figure 5.** (A) Palladium oxide extended gate FET (reprinted from [95] with the permission of Elsevier). (B).  $\text{Na}_3\text{BiO}_4$  and  $\text{Bi}_2\text{O}_3$  ISFET schematics (reprinted from [98] with the permission of Elsevier) (C) Nanocrystalline graphene-based pH sensor (polydimethylsiloxane, PDMS) (reprinted from [99] with the permission of ACS).

Sharma et al. reported a mixed layer of  $\text{Na}_3\text{BiO}_4$  and  $\text{Bi}_2\text{O}_3$  nanostructures on an indium tin oxide electrode (Figure 5B) [98]. This oxide layer allowed for a sensitivity of 49.63 mV/pH in the pH range 7–12. Jung et al. coated an  $\text{SiO}_2$  layer with nanocrystalline graphene that, when exposed to  $\text{H}^+$ , changed its conductivity and allowed for a sensitivity of 140 mV/pH in the pH range 6–7.6 (Figure 5C) [99].

Table 1 summarizes the analytical parameters of the sensors reported in this review.

**Table 1.** Analytical parameters of the cited works. Reproducibility is defined as the relative standard deviation over different sensors. Precision is defined as the RSD on the same sensor.

Transduction	Reproducibility	Precision	Sensitivity	Hysteresis	Interferents	Working Range	Matrix	Response Time	Life Time	Ref
Optical	-	-	-	-	-	2–8	-	1 s	1 month	[23]
Optical	<0.1 pH units	-	-	-	-	6–9	-	180 s	-	[24]
Optical	-	-	-	-	-	7.3–9.3	Marine sediments	200 s	>3 days	[21]
Optical	-	-	-	-	-	6–8	Marine sediments	16 s	1 week	[22]
Optical	<0.20 pH units	0.16 pH units	-	-	-	0–14	-	-	-	[25]
Optical	-	-	-	-	-	6.80–9.00	-	-	-	[26]
Optical	-	-	-	-	-	4–12	Detergent	<5 s	>1 month	[27]
Optical	-	<2%	-	-	-	1–14 with Neural network	-	54 s	-	[28]
Optical	-	<0.3%	-	-	-	0.5–5	-	180 s	>3 months	[29]
Optical	-	-	-	-	Na <sup>+</sup> , K <sup>+</sup> , Ag <sup>+</sup> , Mg <sup>2+</sup> , Ca <sup>2+</sup> , Pb <sup>2+</sup> , Co <sup>2+</sup> , Ni <sup>2+</sup> , Cu <sup>2+</sup> , Zn <sup>2+</sup> , Cd <sup>2+</sup> , Hg <sup>2+</sup> , Al <sup>3+</sup> , Cr <sup>3+</sup> , Fe <sup>3+</sup> , Au <sup>3+</sup> , Pt <sup>2+</sup> , Ru <sup>2+</sup>	1–8	-	-	-	[30]
Optical	-	<1%	6.6 dBm/pH	-	-	1–13	-	40 s	-	[31]
Optical	-	±0.20 pH units	-	-	Ionic Strength	5–8	Human serum	1200 s	>2 months	[33]
Optical	-	<0.1 pH units	-	-	-	4.7–7.7	-	-	-	[34]
Optical	-	-	-	-	-	6–9	-	20 s	-	[35]
Optical	-	-	-	-	-	11–13	-	50 s	>7 months	[36]
Optical	-	-	-	-	-	6–8.5	Subcutaneous tissue	<120 s	28 days	[37]
Optical	-	0.1 pH units	-	-	-	5.5–8	Ovine lung tissue	30 s	-	[38]
Optical	-	-	13 nm/pH	0.5%	-	1–12	-	20 s	10 days	[39]
Optical	-	-	6–42 mV/pH	-	-	2.5–9	-	10 s	-	[40]
Optical	-	-	24.93–11.35 nm/pH	-	-	2.4–11.35	-	-	-	[48]
Optical	4.06%	1.14%	-	-	Ionic Strength	4–8 5–8	-	240 s	>2 months	[49]
Potentiometric	-	-	34–52 mV/pH	-	-	2–11	-	-	-	[51]
Potentiometric	-	-	40–50 mV/pH	-	-	2–11	-	-	>1 month	[52]
Potentiometric	2.4–2.9%	-	56.7–58.6 mV/pH	-	Na <sup>+</sup> , K <sup>+</sup> , Cl <sup>-</sup> , SO <sub>4</sub> <sup>2-</sup>	1–15	Milk, orange juice	<20 s	-	[53]
Potentiometric	0.66%	1.9%	54–56 mV/pH	-	Na <sup>+</sup> , K <sup>+</sup> , Cl <sup>-</sup> , SO <sub>4</sub> <sup>2-</sup>	5.5–8	-	<20 s	-	[54]
Potentiometric	-	-	62.4 mV/pH	5.6 mV	Li <sup>+</sup> , Na <sup>+</sup> , K <sup>+</sup> , Mg <sup>2+</sup> , Ca <sup>2+</sup> , NH <sub>4</sub> <sup>+</sup>	4–10	milk	12.8 s	-	[55]
Potentiometric	2.39%	8%	58.57 mV/pH	12%	-	5.45–8.62	-	45 s	-	[56]
Potentiometric	2.7%	-	58 mV/pH	-	Li <sup>+</sup> , Na <sup>+</sup> , Mg <sup>2+</sup> , Ca <sup>2+</sup> , NH <sub>4</sub> <sup>+</sup> , HCO <sub>3</sub> <sup>-</sup>	1–12	Cola	-	>1 months	[57]

Table 1. Cont.

Transduction	Reproducibility	Precision	Sensitivity	Hysteresis	Interferents	Working Range	Matrix	Response Time	Life Time	Ref
Potentiometric	±1 mV/pH	-	56 mV/pH	±3 mV acid region, ±8 mV basic region	Li <sup>+</sup> , Na <sup>+</sup> , K <sup>+</sup>	2–10	River water, lemon juice	<15 s	-	[58]
Potentiometric	-	-	73 mV/pH	-	-	2–12	-	<10 s	-	[59]
Potentiometric	-	-	58 mV/pH	-	Li <sup>+</sup> , Ca <sup>2+</sup> , Cl <sup>-</sup> , SO <sub>4</sub> <sup>2-</sup>	2–10	-	<2 s	-	[60]
Potentiometric	-	-	377.5 mV/pH	-	-	6.90–8.94	Artificial sea water	-	-	[61]
Potentiometric	-	±0.4 mV/pH	58 mV/pH	-	Li <sup>+</sup> , Na <sup>+</sup> , K <sup>+</sup> , Mg <sup>2+</sup> , Ca <sup>2+</sup> , NH <sub>4</sub> <sup>+</sup>	2.89–9.90	-	10 s	-	[41]
Potentiometric	±2 mV/pH	-	61 mV/pH	-	Na <sup>+</sup> , K <sup>+</sup> , Mg <sup>2+</sup> , Ca <sup>2+</sup> , NH <sub>4</sub> <sup>+</sup>	2–12	Artificial sweat	60 ± 20 s	-	[62]
Potentiometric	-	-	31.8 mV/pH	-	-	4–10	Wound exudate	-	>4 days	[65]
Potentiometric	-	-	53 mV/pH	-	-	4–10	-	-	-	[66]
Potentiometric	5%	5%	45 mV/pH	-	-	4–10	sea water	-	>7 days	[67]
Potentiometric	-	-	4 mV/pH	0.5 mV	Glucose, Urea	6–9	-	5 s	-	[72]
Potentiometric	-	-	44–55 mV/pH	-	Na <sup>+</sup> , K <sup>+</sup>	3–8	-	<3 s	>2 weeks	[73]
Potentiometric	-	-	58.3–60.1 mV/pH	-	Li <sup>+</sup> , Na <sup>+</sup> , K <sup>+</sup>	2–10	Milk, sea water, pineapple juice, vinegar	-	-	[74]
Potentiometric	-	-	46–49 mV/pH	-	-	2–12	-	-	>2 months	[75]
Potentiometric	-	-	58.7 mV/pH	5.6	K <sup>+</sup> , Na <sup>+</sup> , Ca <sup>+</sup> , NH <sub>4</sub> <sup>+</sup>	4–10	Urine, Saliva, Sweat, Tears	5 s	-	[76]
Voltammetric	-	-	58 mV/pH	-	-	1–9	-	-	-	[78]
Voltammetric	-	-	38 mV/pH	-	Mg <sup>+</sup> , Ca <sup>+</sup> , K <sup>+</sup>	6.5–8	Bacteria broth	1.6 s	-	[79]
Voltammetric	<0.8%	±0.09 mV/pH	58 mV/pH	-	-	1–12	-	-	-	[80]
Voltammetric	-	-	65 mV/pH	-	-	2–8	Synthetic saliva and saliva	-	-	[81]
Voltammetric	5%	7%	56 mV/pH	-	Li <sup>+</sup> , Na <sup>+</sup>	2–12	Biological and food matrix	-	>2 months	[82]
Voltammetric	<2%	-	62.7 mV/pH	-	-	5–9	Animal blood	-	-	[83]
Voltammetric	-	-	50 mV/pH	-	-	1–12	-	-	-	[84]
Voltammetric	-	-	63.3 mV/pH	-	Na <sup>+</sup> , K <sup>+</sup> , Dissolved oxygen	0–11	Apple cider vinegar	-	-	[85]
Voltammetric and potentiometric	-	-	52 mV/pH	-	-	1–12	Cola, Milk	-	16 days	[86]
Voltammetric	-	0.5%	32.4 mA/pH 15.9 mA/pH	-	K <sup>+</sup> , Na <sup>+</sup> , Li <sup>+</sup>	2–5.5 5.5–10	-	<8 s	-	[87]

Table 1. Cont.

Transduction	Reproducibility	Precision	Sensitivity	Hysteresis	Interferents	Working Range	Matrix	Response Time	Life Time	Ref
Voltammetric	<3.4%	-	-50.14 $\mu\text{A}/\text{pH cm}^2$ -139.2 $\mu\text{A}/\text{pH cm}^2$	-	-	1–5, 7–11	-	-	-	[88]
Transistor	-	-	58 mV/pH	-	-	2–10	-	-	-	[90]
Transistor	-	-	45.1 mV/pH	24 mV 12 mV	-	-	-	600 s	-	[92]
Transistor	-	-	130 mV/pH	-	-	4–10	-	-	-	[93]
Transistor	-	-	62 mV/pH	7.4 mV	-	2–12	-	-	-	[94]
Transistor	-	-	57 mV/pH	25 mV	-	4–10	-	-	-	[95]
Transistor	-	-	49.63 mV/pH	-	-	7–12	-	-	-	[98]
Transistor	-	-	140 mV/pH	-	-	6–7.6	-	-	-	[99]



## 6. Conclusions and Outlook

The optical pH sensors reported in the literature have achieved high precision, but the working range is often rather narrow, or the linear response is poor. To prevent these drawbacks, the combination of several chromophores can improve performances but at the cost of a more complex fabrication. A major objective emerging from the analysis of the literature is the need for matrices capable of reducing the leakage of the pH-sensitive optical species into the medium. Such research is presently focused on new embedding matrices, such as hydrogels, which would allow for long-lasting sensors for pH monitoring. The choice between optical fibers and planar structures is application oriented. Optical fibers seem more suitable for dynamic sensors with reduced dimensions for in situ measurements. Optical planar structures are being successfully employed mainly for static analysis, where the use of specific equipment (e.g., Charge-Coupled Device cameras) allows for spatial pH measurement.

Potentiometric sensors share the same transduction mechanism with the glass electrode, and they can hardly overcome the limits dictated by Nernst's law. Furthermore, several examples have been reported where the impact of interferents (e.g., cations of alkaline and earth alkaline metals) is hardly removed or not studied at all. So far, PANI is the most used pH-sensitive material because the fabrication of a pH sensor is simplified by the electropolymerization of the monomer onto an electrode. The structure of graphene, on the other hand, allows for easy surface functionalization, improving the sensitivity towards pH.

Voltammetric sensors are an evolution of potentiometric sensors. The literature on this topic is limited and the available studies have shown the importance of designing better electroactive molecules to obtain competitive devices. ISFETs are valid alternative systems to the classical pH measurement methods, capable of overcoming the Nernstian limitation and achieving small dimensional scales thanks to microfabrication procedures. However, the available analytical data are not detailed enough to evaluate their performance, especially in real matrices.

Although glass electrodes are still far from being outdated by new pH sensors, the research for new materials could boost the development of the devices. In particular, a full integration of a reference electrode into an ISFET could pave the way towards a wider use of this technology for pH measurement.

**Funding:** This research was funded by the Italian National Interuniversity Consortium of Materials Science and Technology (INSTM), grant number INSTMPI004.

**Conflicts of Interest:** The authors declare no conflict of interest.

## References

1. Sarkawi, S. An Overview on pH Measurement Technique and Application in Biomedical and Industrial Process. In Proceedings of the 2015 2nd International Conference on Biomedical Engineering (ICoBE), Penang, Malaysia, 30–31 March 2015.
2. Jin, Q.; Kirk, M.F. pH as a Primary Control in Environmental Microbiology: 1. Thermodynamic Perspective. *Front. Environ. Sci.* **2018**, *6*, 21. [[CrossRef](#)]
3. Allen, L.; Ansel, H.C. *Ansel's Pharmaceutical Dosage Forms and Drug Delivery Systems*; Lippincott Williams & Wilkins: Philadelphia, PA, USA, 2013; ISBN 1451188765.
4. Salvo, P.; Dini, V.; Di Francesco, F.; Romanelli, M. The role of biomedical sensors in wound healing. *Wound Med.* **2015**, *8*, 15–18. [[CrossRef](#)]
5. Salvo, P.; Calisi, N.; Melai, B.; Dini, V.; Paoletti, C.; Lomonaco, T.; Pucci, A.; Di Francesco, F.; Piaggese, A.; Romanelli, M. Temperature- and pH-sensitive wearable materials for monitoring foot ulcers. *Int. J. Nanomed.* **2017**, *12*, 949. [[CrossRef](#)] [[PubMed](#)]
6. Zhang, X.; Lin, Y.; Gillies, R.J. Tumor pH and its measurement. *J. Nucl. Med.* **2010**, *51*, 1167–1170. [[CrossRef](#)] [[PubMed](#)]
7. de Lima, T.M.; Kazama, C.M.; Koczulla, A.R.; Hiemstra, P.S.; Macchione, M.; Godoy Fernandes, A.L.; de Paula Santos, U.; Bueno-Garcia, M.L.; Zanetta, D.M.; Saldiva de André, C.D.; et al. PH in exhaled breath condensate and nasal lavage as a biomarker of air pollution-related inflammation in street traffic-controllers and office-workers. *Clinics* **2013**, *68*, 1488–1494. [[CrossRef](#)]
8. Cremer, M. Über die Ursache der elektromotorischen Eigenschaften der Gewebe, zugleich ein Beitrag zur Lehre von polyphasischen Elektrolytketten. *Z. Biol.* **1906**, *47*, 562–608.

9. Leiner, M.J.P.; Hartmann, P. Theory and practice in optical pH sensing. *Sens. Actuators B. Chem.* **1993**. [[CrossRef](#)]
10. Richter, A.; Paschew, G.; Klatt, S.; Lienig, J.; Arndt, K.F.; Adler, H.J.P. Review on hydrogel-based pH sensors and microsensors. *Sensors* **2008**, *8*, 561–581. [[CrossRef](#)]
11. Weston, M.; Kuchel, R.P.; Ciftci, M.; Boyer, C.; Chandrawati, R. A polydiacetylene-based colorimetric sensor as an active use-by date indicator for milk. *J. Colloid Interface Sci.* **2020**, *572*, 31–38. [[CrossRef](#)]
12. Yuqing, M.; Jianrong, C.; Keming, F. New technology for the detection of pH. *J. Biochem. Biophys. Methods* **2005**, *63*, 1–9. [[CrossRef](#)]
13. Salvo, P.; Melai, B.; Calisi, N.; Paoletti, C.; Bellagambi, F.; Kirchhain, A.; Trivella, M.G.; Fuoco, R.; Di Francesco, F. Graphene-based devices for measuring pH. *Sens. Actuators B Chem.* **2018**, *256*, 976–991. [[CrossRef](#)]
14. Wencel, D.; Abel, T.; McDonagh, C. Optical chemical pH sensors. *Anal. Chem.* **2014**, *86*, 15–29. [[CrossRef](#)]
15. Baldini, F. Critical review of pH sensing with optical fibres. In *Chemical, Biochemical, and Environmental Fiber Sensors X*; International Society for Optics and Photonics: Bellingham, WA, USA, 1999; Volume 3540, pp. 2–9.
16. Butler, T.M.; MacCraith, B.D.; McDonagh, C. Leaching in sol-gel-derived silica films for optical pH sensing. *J. Non. Cryst. Solids* **1998**, *224*, 249–258. [[CrossRef](#)]
17. Lev, O.; Tsionsky, M.; Rabinovich, L.; Glezer, V.; Sampath, S.; Pankratov, I.; Gun, J. Organically Modified Sol-Gel Sensors. *Anal. Chem.* **1995**, *67*, 22A–30A. [[CrossRef](#)]
18. Plaschke, M.; Czolk, R.; Ache, H.J. Fluorimetric determination of mercury with a water-soluble porphyrin and porphyrin-doped sol-gel films. *Anal. Chim. Acta* **1995**, *304*, 107–113. [[CrossRef](#)]
19. Zhu, Q.; Aller, R.C. Planar fluorescence sensors for two-dimensional measurements of H<sub>2</sub>S distributions and dynamics in sedimentary deposits. *Mar. Chem.* **2013**. [[CrossRef](#)]
20. Zhu, Q.; Aller, R.C.; Fan, Y. High-performance planar pH fluorosensor for two-dimensional pH measurements in marine sediment and water. *Environ. Sci. Technol.* **2005**, *39*, 8906–8911. [[CrossRef](#)] [[PubMed](#)]
21. Stahl, H.; Glud, A.; Schröder, C.R.; Klimant, I.; Tengberg, A.; Glud, R.N. Time-resolved pH imaging in marine sediments with a luminescent planar optode. *Limnol. Oceanogr. Methods* **2006**, *4*, 336–345. [[CrossRef](#)]
22. Jiang, Z.; Yu, X.; Hao, Y. Design and fabrication of a ratiometric planar optode for simultaneous imaging of pH and oxygen. *Sensors* **2017**, *17*, 1316. [[CrossRef](#)]
23. Jin, Z.; Su, Y.; Duan, Y. An improved optical pH sensor based on polyaniline. *Sens. Actuators B Chem.* **2000**, *71*, 118–122. [[CrossRef](#)]
24. Kermis, H.R.; Kostov, Y.; Rao, G. Rapid method for the preparation of a robust optical pH sensor. *Analyst* **2003**, *128*, 1181–1186. [[CrossRef](#)] [[PubMed](#)]
25. Gotor, R.; Ashokkumar, P.; Hecht, M.; Keil, K.; Rurack, K. Optical pH Sensor Covering the Range from pH 0–14 Compatible with Mobile-Device Readout and Based on a Set of Rationally Designed Indicator Dyes. *Anal. Chem.* **2017**, *89*, 8437–8444. [[CrossRef](#)] [[PubMed](#)]
26. Raoufi, N.; Surre, F.; Sun, T.; Rajarajan, M.; Grattan, K.T.V. Wavelength dependent pH optical sensor using the layer-by-layer technique. *Sens. Actuators, B Chem.* **2012**, *169*, 374–381. [[CrossRef](#)]
27. Abu-Thabit, N.; Umar, Y.; Ratemi, E.; Ahmad, A.; Abuilaiwi, F.A. A flexible optical pH sensor based on polysulfone membranes coated with pH-responsive polyaniline nanofibers. *Sensors* **2016**, *16*, 986. [[CrossRef](#)] [[PubMed](#)]
28. Safavi, A.; Bagheri, M. Novel optical pH sensor for high and low pH values. *Sens. Actuators B Chem.* **2003**, *90*, 143–150. [[CrossRef](#)]
29. Hashemi, P.; Abolghasemi, M.M. Preparation of a novel optical sensor for low pH values using agarose membranes as support. *Sens. Actuators B Chem.* **2006**, *115*, 49–53. [[CrossRef](#)]
30. Taweetanavanich, T.; Wannoo, B.; Tuntulani, T.; Pulpoka, B.; Kaewtong, C. A pH optical and fluorescent sensor based on rhodamine modified on activated cellulose paper. *J. Chinese Chem. Soc.* **2019**, *66*, 493–499. [[CrossRef](#)]
31. Li, W.; Cheng, H.; Xia, M.; Yang, K. An experimental study of pH optical sensor using a section of no-core fiber. *Sens. Actuators A Phys.* **2013**, *199*, 260–264. [[CrossRef](#)]
32. Jung, Y.; Kim, S.; Lee, D.; Oh, K. Compact three segmented multimode fibre modal interferometer for high sensitivity refractive-index measurement. *Meas. Sci. Technol.* **2006**, *17*, 1129. [[CrossRef](#)]
33. Schyrr, B.; Pasche, S.; Scolan, E.; Ischer, R.; Ferrario, D.; Porchet, J.A.; Voirin, G. Development of a polymer optical fiber pH sensor for on-body monitoring application. *Sens. Actuators B Chem.* **2014**, *194*, 238–248. [[CrossRef](#)]
34. Sørensen, T.J.; Rosenberg, M.; Frankær, C.G.; Laursen, B.W. An Optical pH Sensor Based on Diazaoxatriangulenium and Isopropyl-Bridged Diazatriangulenium Covalently Bound in a Composite Sol–Gel. *Adv. Mater. Technol.* **2019**. [[CrossRef](#)]
35. Jeon, D.; Yoo, W.J.; Seo, J.K.; Shin, S.H.; Han, K.T.; Kim, S.G.; Park, J.Y.; Lee, B. Fiber-optic pH sensor based on sol-gel film immobilized with neutral red. *Opt. Rev.* **2013**, *20*, 209–213. [[CrossRef](#)]
36. Mahboubeh, V.; Rounaghi, G.H.; Es'haghi, Z.; Moradi, Z. Design and Application of an Optical pH Sensor Based on Thionine Doped Modified Sol–Gel Film. *Russ. J. Phys. Chem. A* **2019**, *93*, 1389–1393. [[CrossRef](#)]
37. Wencel, D.; Kaworek, A.; Abel, T.; Efremov, V.; Bradford, A.; Carthy, D.; Coady, G.; McMorro, R.C.N.; McDonagh, C. Optical Sensor for Real-Time pH Monitoring in Human Tissue. *Small* **2018**, *14*, 1–8. [[CrossRef](#)]
38. Gong, J.; Tanner, M.G.; Venkateswaran, S.; Stone, J.M.; Zhang, Y.; Bradley, M. A hydrogel-based optical fibre fluorescent pH sensor for observing lung tumor tissue acidity. *Anal. Chim. Acta* **2020**, *1134*, 136–143. [[CrossRef](#)]
39. Zhao, Y.; Lei, M.; Liu, S.X.; Zhao, Q. Smart hydrogel-based optical fiber SPR sensor for pH measurements. *Sens. Actuators, B Chem.* **2018**, *261*, 226–232. [[CrossRef](#)]

40. Moradi, V.; Akbari, M.; Wild, P. A fluorescence-based pH sensor with microfluidic mixing and fiber optic detection for wide range pH measurements. *Sens. Actuators A Phys.* **2019**, *297*, 111507. [[CrossRef](#)]
41. Crespo, G.A.; Gugsá, D.; MacHo, S.; Rius, F.X. Solid-contact pH-selective electrode using multi-walled carbon nanotubes. *Anal. Bioanal. Chem.* **2009**, *395*, 2371–2376. [[CrossRef](#)]
42. Gill, E.; Arshak, K.; Arshak, A.; Korostyńska, O. Mixed metal oxide films as pH sensing materials. *Microsyst. Technol.* **2008**, *14*, 499–507. [[CrossRef](#)]
43. Fog, A.; Buck, R.P. Electronic semiconducting oxides as pH sensors. *Sens. Actuators* **1984**, *5*, 137–146. [[CrossRef](#)]
44. Manjakkal, L.; Szwagierczak, D.; Dahiya, R. Metal oxides based electrochemical pH sensors: Current progress and future perspectives. *Prog. Mater. Sci.* **2020**, *109*, 100635. [[CrossRef](#)]
45. Wei, A.; Pan, L.; Huang, W. Recent progress in the ZnO nanostructure-based sensors. *Mater. Sci. Eng. B Solid-State Mater. Adv. Technol.* **2011**, *176*, 1409–1421. [[CrossRef](#)]
46. Huang, X.J.; Choi, Y.K. Chemical sensors based on nanostructured materials. *Sens. Actuators B Chem.* **2007**, *122*, 659–671. [[CrossRef](#)]
47. Gláb, S.; Hulanicki, A.; Edwall, G.; Folke, F.; Ingman, I.; Koch, W.F. Metal-Metal Oxide and Metal Oxide Electrodes as pH Sensors. *Crit. Rev. Anal. Chem.* **1989**, *21*, 29–47. [[CrossRef](#)]
48. Semwal, V.; Gupta, B.D. Highly sensitive surface plasmon resonance based fiber optic pH sensor utilizing rGO-Pani nanocomposite prepared by in situ method. *Sens. Actuators B Chem.* **2019**, *283*, 632–642. [[CrossRef](#)]
49. Shahamirifard, S.A.; Ghaedi, M.; Montazerzohori, M. Application of nanostructure ZnLI2 complex in construction of optical pH sensor. *Appl. Organomet. Chem.* **2018**, *32*, 1–11. [[CrossRef](#)]
50. Bobacka, J.; Ivaska, A.; Lewenstam, A. Potentiometric ion sensors. *Chem. Rev.* **2008**, *108*, 329–351. [[CrossRef](#)] [[PubMed](#)]
51. Lakard, B.; Herlem, G.; Lakard, S.; Guyetant, R.; Fahys, B. Potentiometric pH sensors based on electrodeposited polymers. *Polymer* **2005**, *46*, 12233–12239. [[CrossRef](#)]
52. Lakard, B.; Segut, O.; Lakard, S.; Herlem, G.; Gharbi, T. Potentiometric miniaturized pH sensors based on polypyrrole films. *Sens. Actuators, B Chem.* **2007**, *122*, 101–108. [[CrossRef](#)]
53. Li, Q.; Li, H.; Zhang, J.; Xu, Z. A novel pH potentiometric sensor based on electrochemically synthesized polybisphenol A films at an ITO electrode. *Sens. Actuators B Chem.* **2011**, *155*, 730–736. [[CrossRef](#)]
54. Guinovart, T.; Valdés-Ramírez, G.; Windmiller, J.R.; Andrade, F.J.; Wang, J. Bandage-Based Wearable Potentiometric Sensor for Monitoring Wound pH. *Electroanalysis* **2014**, *26*, 1345–1353. [[CrossRef](#)]
55. Park, H.J.; Yoon, J.H.; Lee, K.G.; Choi, B.G. Potentiometric performance of flexible pH sensor based on polyaniline nanofiber arrays. *Nano Converg.* **2019**, *6*. [[CrossRef](#)]
56. Li, Y.; Mao, Y.; Xiao, C.; Xu, X.; Li, X. Flexible pH sensor based on a conductive PANI membrane for pH monitoring. *RSC Adv.* **2019**, *10*, 21–28. [[CrossRef](#)]
57. Eftekhari, A. pH sensor based on deposited film of lead oxide on aluminum substrate electrode. *Sens. Actuators B Chem.* **2003**, *88*, 234–238. [[CrossRef](#)]
58. Manjakkal, L.; Zaraska, K.; Cvejín, K.; Kulawik, J.; Szwagierczak, D. Potentiometric RuO<sub>2</sub>-Ta<sub>2</sub>O<sub>5</sub> pH sensors fabricated using thick film and LTCC technologies. *Talanta* **2016**, *147*, 233–240. [[CrossRef](#)]
59. Khalil, M.; Liu, N.; Lee, R.L. Super-Nernstian potentiometric pH sensor based on the electrodeposition of iridium oxide nanoparticles. *Int. J. Technol.* **2018**, *57*, 446–454. [[CrossRef](#)]
60. Tanumihardja, E.; Olthuis, W.; van den Berg, A. Ruthenium oxide nanorods as potentiometric pH sensor for organs-on-chip purposes. *Sensors* **2018**, *18*, 2901. [[CrossRef](#)] [[PubMed](#)]
61. Choi, S.J.; Savagatrup, S.; Kim, Y.; Lang, J.H.; Swager, T.M. Precision pH Sensor Based on WO<sub>3</sub> Nanofiber-Polymer Composites and Differential Amplification. *ACS Sens.* **2019**, *4*, 2593–2598. [[CrossRef](#)] [[PubMed](#)]
62. Smith, R.E.; Totti, S.; Velliou, E.; Campagnolo, P.; Hingley-Wilson, S.M.; Ward, N.I.; Varcoe, J.R.; Crean, C. Development of a novel highly conductive and flexible cotton yarn for wearable pH sensor technology. *Sens. Actuators B Chem.* **2019**, *287*, 338–345. [[CrossRef](#)]
63. Salvo, P.; Calisi, N.; Melai, B.; Cortigiani, B.; Mannini, M.; Caneschi, A.; Lorenzetti, G.; Paoletti, C.; Lomonaco, T.; Paolicchi, A.; et al. Temperature and pH sensors based on graphenic materials. *Biosens. Bioelectron.* **2017**, *91*, 870–877. [[CrossRef](#)]
64. Salvo, P.; Dini, V.; Kirchhain, A.; Janowska, A.; Oranges, T.; Chiricozzi, A.; Lomonaco, T.; Di Francesco, F.; Romanelli, M. Sensors and biosensors for C-reactive protein, temperature and pH, and their applications for monitoring wound healing: A review. *Sensors* **2017**, *17*, 2952. [[CrossRef](#)]
65. Melai, B.; Salvo, P.; Calisi, N.; Moni, L.; Bonini, A.; Paoletti, C.; Lomonaco, T.; Mollica, V.; Fuoco, R.; Di Francesco, F. A graphene oxide pH sensor for wound monitoring. In Proceedings of the 2016 38th Annual International Conference of the IEEE Engineering in Medicine and Biology Society (EMBC), Orlando, FL, USA, 16–20 August 2016; pp. 1898–1901.
66. Rahimi, R.; Ochoa, M.; Tamayol, A.; Khalili, S.; Khademhosseini, A.; Ziaie, B. Highly Stretchable Potentiometric pH Sensor Fabricated via Laser Carbonization and Machining of Carbon–Polyaniline Composite. *ACS Appl. Mater. Interfaces* **2017**, *9*, 9015–9023. [[CrossRef](#)]
67. Poma, N.; Vivaldi, F.; Bonini, A.; Carbonaro, N.; Di Rienzo, F.; Melai, B.; Kirchhain, A.; Salvo, P.; Tognetti, A.; Di Francesco, F. Remote monitoring of seawater temperature and pH by low cost sensors. *Microchem. J.* **2019**, *148*, 248–252. [[CrossRef](#)]

68. Bonini, A.; Di Francesco, F.; Salvo, P.; Vivaldi, F.; Herrera, E.; Melai, B.; Kirchhain, A.; Poma, N.; Mattonai, M.; Caprioli, R.; et al. A Graphenic Biosensor for Real-Time Monitoring of Urea during Dialysis. *IEEE Sens. J.* **2020**. [[CrossRef](#)]
69. Herrera, E.G.; Bonini, A.; Vivaldi, F.; Melai, B.; Salvo, P.; Poma, N.; Santalucia, D.; Kirchhain, A.; Di Francesco, F. A Biosensor for the Detection of Acetylcholine and Diazinon. *Proc. Annu. Int. Conf. IEEE Eng. Med. Biol. Soc. EMBS* **2019**, 1159–1162. [[CrossRef](#)]
70. Poma, N.; Vivaldi, F.; Bonini, A.; Salvo, P.; Kirchhain, A.; Melai, B.; Bottai, D.; Tavanti, A.; Di Francesco, F. A graphenic and potentiometric sensor for monitoring the growth of bacterial biofilms. *Sens. Actuators B Chem.* **2020**. [[CrossRef](#)]
71. Vivaldi, F.; Bonini, A.; Melai, B.; Poma, N.; Kirchhain, A.; Santalucia, D.; Salvo, P.; Di Francesco, F. A graphene-based pH sensor on paper for human plasma and seawater. In Proceedings of the 2019 41st Annual International Conference of the IEEE Engineering in Medicine and Biology Society (EMBC), Berlin, Germany, 23–27 July 2019; pp. 1563–1566. [[CrossRef](#)]
72. Manjakkal, L.; Dang, W.; Yogeswaran, N.; Dahiya, R. Textile-based potentiometric electrochemical PH sensor for wearable applications. *Biosensors* **2019**, *9*, 14. [[CrossRef](#)]
73. Marxer, S.M.; Schoenfisch, M.H. Sol-gel derived potentiometric pH sensors. *Anal. Chem.* **2005**, *77*, 848–853. [[CrossRef](#)] [[PubMed](#)]
74. Zuaznabar-Gardona, J.C.; Fragoso, A. A wide-range solid state potentiometric pH sensor based on poly-dopamine coated carbon nano-onion electrodes. *Sens. Actuators B Chem.* **2018**, *273*, 664–671. [[CrossRef](#)]
75. Sulka, G.D.; Hnida, K.; Agnieszka Brzózka, A. PH sensors based on polypyrrole nanowire arrays. *Electrochim. Acta* **2013**, *104*, 536–541. [[CrossRef](#)]
76. Yoon, J.H.; Kim, S.M.; Park, H.J.; Kim, Y.K.; Oh, D.X.; Cho, H.W.; Lee, K.G.; Hwang, S.Y.; Park, J.; Choi, B.G. Highly self-healable and flexible cable-type pH sensors for real-time monitoring of human fluids. *Biosens. Bioelectron.* **2020**, *150*, 111946. [[CrossRef](#)] [[PubMed](#)]
77. Stred'Anský, M.; Pizzariello, A.; Stred'Anská, S.; Miertuš, S. Amperometric pH-sensing biosensors for urea, penicillin, and oxalacetate. *Anal. Chim. Acta* **2000**, *415*, 151–157. [[CrossRef](#)]
78. Wildgoose, G.G.; Pandurangappa, M.; Lawrence, N.S.; Jiang, L.; Jones, T.G.J.; Compton, R.G. Anthraquinone-derivatised carbon powder: Reagentless voltammetric pH electrodes. *Talanta* **2003**, *60*, 887–893. [[CrossRef](#)]
79. Makos, M.A.; Omiatek, D.M.; Ewing, A.G.; Heien, M.L. Development and characterization of a voltammetric carbon-fiber microelectrode pH sensor. *Langmuir* **2010**, *26*, 10386–10391. [[CrossRef](#)] [[PubMed](#)]
80. Amiri, M.; Amali, E.; Nematollahzadeh, A.; Salehniya, H. Poly-dopamine films: Voltammetric sensor for pH monitoring. *Sens. Actuators B Chem.* **2016**, *228*, 53–58. [[CrossRef](#)]
81. Chaisiwamongkhol, K.; Batchelor-Mcauley, C.; Compton, R.G. Amperometric micro pH measurements in oxygenated saliva. *Analyst* **2017**, *142*, 2828–2835. [[CrossRef](#)]
82. Vivaldi, F.; Santalucia, D.; Poma, N.; Bonini, A.; Salvo, P.; Del Noce, L.; Melai, B.; Kirchhain, A.; Kolivoška, V.; Sokolová, R.; et al. A voltammetric pH sensor for food and biological matrices. *Sens. Actuators B Chem.* **2020**. [[CrossRef](#)]
83. Chaisiwamongkhol, K.; Batchelor-Mcauley, C.; Compton, R.G. Optimising amperometric pH sensing in blood samples: An iridium oxide electrode for blood pH sensing. *Analyst* **2019**, *144*, 1386–1393. [[CrossRef](#)]
84. Tham, G.X.; Fisher, A.C.; Webster, R.D. A vitamin-based voltammetric pH sensor that functions in buffered and unbuffered media. *Sens. Actuators B Chem.* **2019**, *283*, 495–503. [[CrossRef](#)]
85. Zhu, H.; Hassan, T.; Kabir, H.; May, J.; Hamal, K.; Lopez, R.; Smith, H.J.; Nicholas, N.W.; Sankaran, P.; McIlroy, D.N.; et al. Voltammetric pH sensor based on electrochemically modified pseudo-graphite. *Analyst* **2020**, *145*, 7252–7259. [[CrossRef](#)] [[PubMed](#)]
86. Hu, G.; Li, N.; Zhang, Y.; Li, H. A novel pH sensor with application to milk based on electrochemical oxidative quinone-functionalization of tryptophan residues. *J. Electroanal. Chem.* **2020**, *859*, 113871. [[CrossRef](#)]
87. Gao, W.; Song, J. Polyaniline film based amperometric pH sensor using a novel electrochemical measurement system. *Electroanalysis* **2009**, *21*, 973–978. [[CrossRef](#)]
88. Sha, R.; Komori, K.; Badhulika, S. Amperometric pH Sensor Based on Graphene-Polyaniline Composite. *IEEE Sens. J.* **2017**, *17*, 5038–5043. [[CrossRef](#)]
89. Bergveld, P. Development of an Ion-Sensitive Solid-State Device for Neurophysiological Measurements. *IEEE Trans. Biomed. Eng.* **1970**, *BME-17*, 70–71. [[CrossRef](#)]
90. Chin, Y.L.; Chou, J.C.; Sun, T.P.; Liao, H.K.; Chung, W.Y.; Hsiung, S.K. A novel SnO<sub>2</sub>/Al discrete gate ISFET pH sensor with CMOS standard process. *Sens. Actuators B Chem.* **2001**, *75*, 36–42. [[CrossRef](#)]
91. Shitashima, K.; Kyo, M.; Koike, Y.; Henmi, H. Development of in situ pH sensor using ISFET Environmental Science Department. In Proceedings of the 2002 International Symposium on Underwater Technology (Cat. No.02EX556), Tokyo, Japan, 19 April 2002; pp. 106–108. [[CrossRef](#)]
92. Fukuba, T.; Tamai, Y.; Kyo, M.; Shitashima, K.; Koike, Y.; Fujii, T. Development and field evaluation of ISFET pH sensor integrated with self-calibration device for deep-sea oceanography applications. In Proceedings of the 12th International Conference on Miniaturized Systems for Life Sciences, San Diego, CA, USA, 12–16 October 2008; pp. 1983–1985.
93. Rani, R.A.; Syono, M.I.; Ramli, A.S. Multi-finger gate ISFET (Mf-ISFET) for pH sensor application. In Proceedings of the 2008 IEEE International Conference on Semiconductor Electronics, Johor Bahru, Malaysia, 25–27 November 2008; pp. 350–353. [[CrossRef](#)]
94. Parizi, K.B.; Yeh, A.J.; Poon, A.S.Y.; Wong, H.S.P. Exceeding Nernst limit (59mV/pH): CMOS-based pH sensor for autonomous applications. In Proceedings of the 2012 International Electron Devices Meeting, San Francisco, CA, USA, 10–13 December 2012. [[CrossRef](#)]



95. Das, A.; Ko, D.H.; Chen, C.H.; Chang, L.B.; Lai, C.S.; Chu, F.C.; Chow, L.; Lin, R.M. Highly sensitive palladium oxide thin film extended gate FETs as pH sensor. *Sens. Actuators B Chem.* **2014**, *205*, 199–205. [[CrossRef](#)]
96. Cho, W.J.; Lim, C.M. Sensing properties of separative paper-based extended-gate ion-sensitive field-effect transistor for cost effective pH sensor applications. *Solid. State. Electron.* **2018**, *140*, 96–99. [[CrossRef](#)]
97. Kang, T.; Lee, I.; Oh, S.; Jang, T.; Kim, Y.; Ahn, H.; Kim, G.; Shin, S.U.; Jeong, S.; Sylvester, D.; et al. A 1.74.12 mm<sup>3</sup> Fully Integrated pH Sensor for Implantable Applications using Differential Sensing and Drift-Compensation. In Proceedings of the 2019 Symposium on VLSI Circuits, Kyoto, Japan, 9–14 June 2019. [[CrossRef](#)]
98. Sharma, P.; Gupta, S.; Singh, R.; Ray, K.; Kothari, S.L.; Sinha, S.; Sharma, R.; Mukhiya, R.; Awasthi, K.; Kumar, M. Hydrogen ion sensing characteristics of Na<sub>3</sub>BiO<sub>4</sub>–Bi<sub>2</sub>O<sub>3</sub> mixed oxide nanostructures based EGFET pH sensor. *Int. J. Hydrogen Energy* **2020**, *45*, 18743–18751. [[CrossRef](#)]
99. Jung, S.H.; Seo, Y.M.; Gu, T.; Jang, W.; Kang, S.G.; Hyeon, Y.; Hyun, S.H.; Lee, J.H.; Whang, D. Super-Nernstian pH Sensor Based on Anomalous Charge Transfer Doping of Defect-Engineered Graphene. *Nano Lett.* **2020**, *21*, 34–42. [[CrossRef](#)] [[PubMed](#)]